CENTER FOR RESEARCH IN
ENGINEERING AND TECHNOLOGY EDUCATION

SHPE // MAES
UNIVERSITY OF TEXAS AT EL PASO

WELCOME

Miner Spark Symposium

WHERE INNOVATION MEETS CREATIVITY

Who are we?

We are a research program dedicated to helping undergraduate students take their first steps beyond the classroom. Our mission is to provide early support and guidance, enabling students to ignite their curiosity and showcase their spark in research.

Agenda

Team 1

SOIL CORROSION RISK ANALYSIS

Using GIS to model soil corrosion risk in northeast El Paso according to AWWA standards

Authors

G. Yared Rodríguez, NataliaHernandez,Diego Peña, Luisa Cardoso

Affiliations

University ofTexasatElPaso-SHPE//MAES

Introduction

Research Question:What local soil factors contribute to the ***corrosion*** of steel pipes?

On January 11, 2026, a water main break in northeast El Paso left over 100,000 individuals without water and drained ~15 reservoirs. ***AWWA C105*** provides an additive point-score system that evaluates resistivity, pH, redox potential, sulfides, and moisture to assess ***corrosion*** risk. A score of 10 or higher indicates increased risk.
This project applies that standard in Northeast El Paso, using ***GIS*** interpolation to map corrosion risk near January 11's main failure.

Methodology

1. Collected 30 soil samples (depth: to 35 cm) along public right-of-way within a 0.75 km buffer of the January 2026 main break site (~250 m spacing).
2. Measured EC, pH, and ORP with calibrated meters in 1:1 soil-to-distilled-water slurries; tested sulfides with lead acetate paper; drainage visually scored.
3. Converted EC into resistivity and scored all 5 variables per AWWA C105 Appendix A.
4. Interpolated each variable using ***Inverse Distance Weighting*** at power = 2, nearest points = 6, and cell size = 13 m in *ArcGIS Pro* and *ModelBuilder*.
5. Summed reclassified rasters via raster calculator according to AWWA C105 in ModelBuilder.

Objective

To develop a GIS-based visual aidfor corrosion risk analysis according to AWWA C105 Appendix A's standard, and to evaluate whether local conditions pose a measurable corrosion risk to buried steel infrastructure.

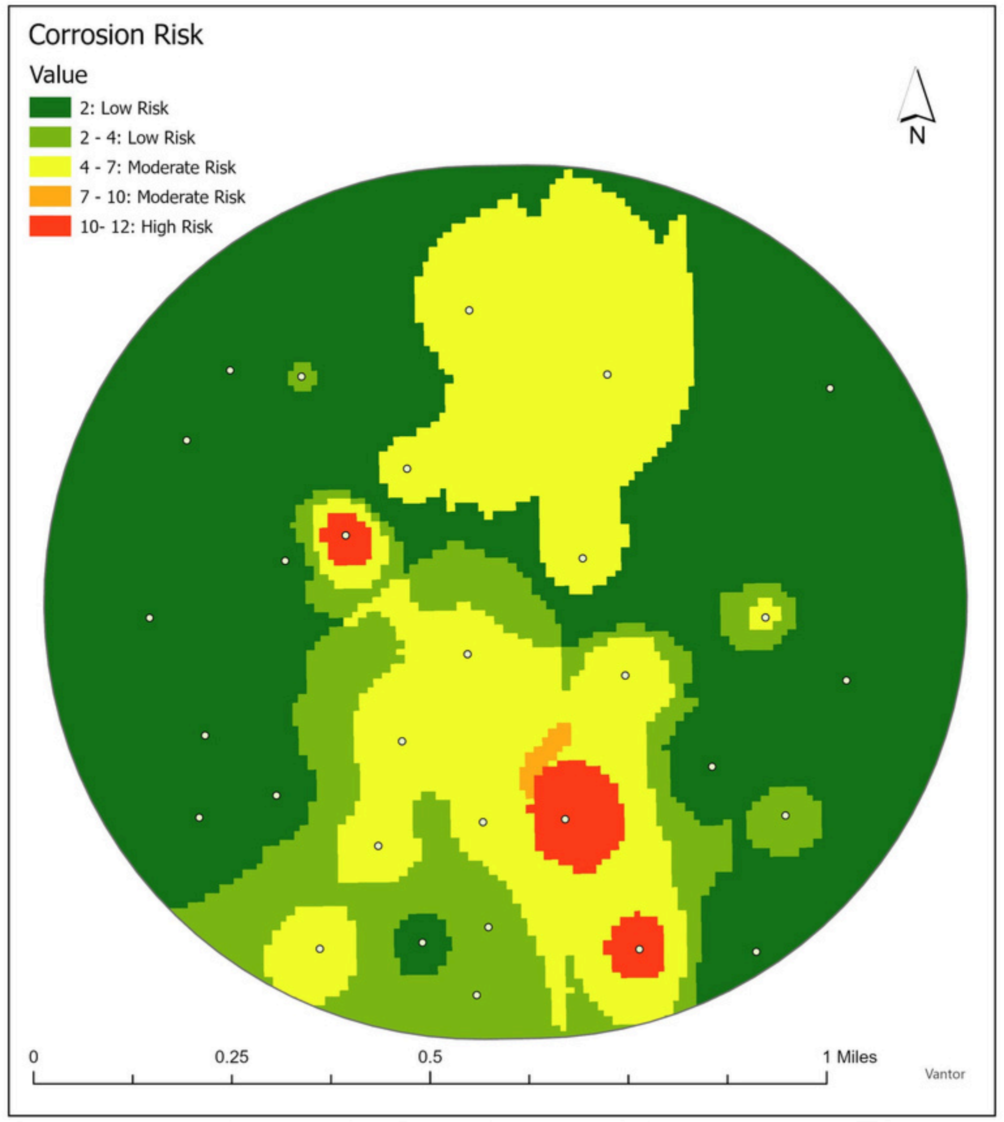

Sources: Field-collected soil samples (n=30), AWWA C105 Appendix A scoring, IDW interpolation in ArcGIS Pro; Basemap: Esri World Imagery. Map by: Gerardo Yared Rodriguez, UTEP. Date: 2026-04-28

Results

AWWA scores ranged from 2 to 12 with ***three high-risk zones*** corresponding to low resistivity and poor drainage near canal infrastructure. Resistivity was the only AWWA variable that produced meaningful score variation (882–23,810 ohm-cm). *pH, ORP, and sulfides scored 0 across all 30 samples.*

El Paso's arid, alkaline soils render three of AWWA's five variables effectively inert.

Limitations

Using a 1:1 soil slurry for resistivity and ORP was a major compromise; AWWA calls for ***in-situ***, but we did not find the equipment needed on-campus.

Steel pipes typically sit at depths of 100 to 200 cm, so specialized probes are used to sample at those depths, but we did not have access to one.

IDW becomes more reliable with more points. At this resolution, 30 is fine but with more time we would have done 50.

Conclusion

Most of our interest area scored belowAWWA's threshold, but three zones exceeded it. Of AWWA's variables, only moisture and resistivity were significant within our area of interest. In El Paso, pH has a bigger role near the acidic river valley, and with better testing methods ORP would be a real factor everywhere. Future work should expand sampling into the river valley's more variable soils with ***in-situ*** methods to activate the three AWWA parameters that were inert in this environment.

Key Sources & Acknowledgements

- AWWA (2018). ANSI/AWWA C105/A21.5-18. American Water Works Association.
- Arriba-Rodriguez, L. et al. (2018). Methods to evaluate corrosion in buried steel structures: A review. Metals, 8(5).
- Georgiou, N. et al. (2016). Classification of corrosion risk zones using GIS. Fourth Int. Conf. on Remote Sensing and Geoinformation (RSCy2016).

Thank you to the Miner Spark team and CrEATE for their support, and a special thank you to Adelaide Rodriguez, MSGIS at ASU, for her guidance on GIS workflows.

Q&A

Team 2

4D-Printed Materials for Manufacturing: A Study of Thermal and Mechanical Performance

AnelGaytan[1], AbrilSalcido[2], OscarSalais[2], EduardoMoyer[3]
The University of Texas at El Paso: Department of Engineering
[1]University of Texas at El Paso (UTEP): Department of Electrical & Computer Engineering
[2]University of Texas at El Paso (UTEP): Department of Aerospace & Mechanical Engineering
[3]University of Texas at El Paso (UTEP): Department of Computer Science

INTRODUCTION

Shape memory polymers (SMPs) are smart materials capable of returning to a predefined shape when exposed to heat, making them promising for adaptive manufacturing applications. In contrast, polylactic acid (PLA), a common 3D printing material, provides structural stability but does not exhibit shape memory behavior. This study compares SMP and PLA under thermal and mechanical conditions using multiple geometries. Samples were subjected to controlled heating and applied loads to evaluate deformation and recovery behavior. These results provide insight into the feasibility of using 4D-printed materials in real-world manufacturing applications.

MATERIALS & METHODS

Test Materials

- Shape Memory Polymer (SMP)
- Polylactic Acid (PLA)

Sample Design

- Geometries: Cube, Triangle (Pyramid), Sphere
- All samples were 3D printed using both materials for direct comparison

Independent Variables:

- Material type (SMP vs PLA)
- Geometry
- Temperature (~65°C)
- Applied load (0–30 g)

Measured Outcomes:

- Degree of deformation
- Final recovered height
- Shape recovery quality

Procedure

Samples were 3D printed in SMP and PLA using identical geometries (cube, triangle, and sphere) to ensure direct comparison. SMP samples were programmed by heating above their activation temperature (~65°C), deforming into a temporary shape, and cooling below ~30°C to fix that shape. A heated water bath (~65°C) was maintained to provide consistent thermal activation across all trials. Samples were submerged in the water bath and positioned consistently to ensure uniform exposure. External loads (0 g, 20 g, and 30 g) were applied to simulate mechanical stress. All samples were exposed for a consistent duration to ensure full thermal response and recovery. After heating, samples were removed, stabilized, and measured. Final height and shape were recorded to evaluate deformation and recovery. PLA samples were tested under identical conditions for direct comparison with SMP.

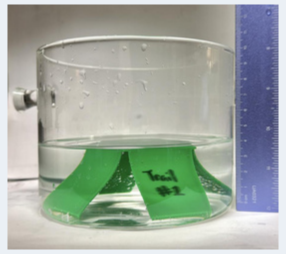

RESULTS

SMP samples demonstrated strong and consistent shape recovery across all geometries. At lower loads (0–20 g), recovery heights approached the original 5.0 cm, with values reaching approximately 4.3–4.7 cm. As load increased to 30 g, recovery decreased but remained significantly higher than PLA, indicating strong structural stability under stress.

Across geometries, the sphere and cube showed the highest recovery, while the triangle exhibited slightly lower performance under higher loads. Overall, SMP maintained repeatable and smooth recovery behavior with minimal structural degradation.

Table 1:SMP Temperature vs. Weight vs. Height Change
Original Height: 5.0cm

Trial (#) and Temperature (°C)	Weight (g)	Molded Height (cm)	Recovery Height (cm)	△Height (cm)	Percent Error (%)
Trial 0 / 65°	0g	1.5cm	4.3cm	0.7cm	16.28%
CUBE Trial 1 / 65° Trial 2 / 65°	20g 30g	2.35cm 1.4cm	3.6cm 3.5cm	1.4cm 2.1cm	39.9% 42.9%
TRIANGLE Trial 1 / 65° Trial 2 / 65°	20g 30g	1.4cm 1.4cm	2.5cm 2.4cm	1.1cm 1.0cm	100% 108.3%
SPHERE Trial 1 / 65° Trial 2 / 65°	20g 30g	1.4cm 1.4cm	4.5cm 3.0cm	3.1cm 1.6cm	11.1% 67.7%

PLA samples showed significant deformation when exposed to heat but did not consistently recover their original shape. While some recovery was observed at lower loads, performance became increasingly inconsistent as load increased. At 30 g, recovery dropped substantially, with some samples reaching only ~2.8–3.0 cm. Unlike SMP, PLA exhibited uneven deformation across geometries, with visible instability and variation in recovery height. This indicates that PLA lacks the ability to reliably return to its original shape under combined thermal and mechanical conditions.

Table 2: PLA Temperature vs. Weight vs. Height Change
Original Height: 5.0cm

Trail (#) and Temperature (°C)	Weight (g)	Molded Height (cm)	Recovery Height (cm)	△Height (cm)	Percent Error (%)
CUBE Trial 1 / 65° Trial 2 / 65°	20g 30g	1.4cm 1.4cm	4.7cm 4.4cm	0.3cm 0.6cm	6.40% 13.60%
TRIANGLE Trial 1 / 65° Trial 2 / 65°	20g 30g	1.4cm 1.4cm	4.5cm 4.2cm	0.5cm 0.8cm	11.0% 19.1%
SPHERE Trial 1 / 65° Trial 2 / 65°	20g 30g	1.4cm 1.4cm	4.3cm 2.8cm	0.7cm 1.2cm	16.30% 78.60%

FIGURES

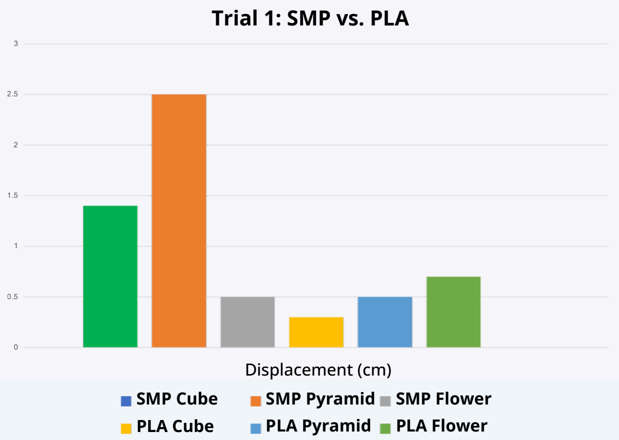

In Trial 1, SMP demonstrates significantly greater recovery displacement than PLA across all geometries. The cube and pyramid shapes show the largest differences, with SMP achieving substantially higher recovery values while PLA remains limited. This indicates strong initial recovery performance and structural stability in SMP.

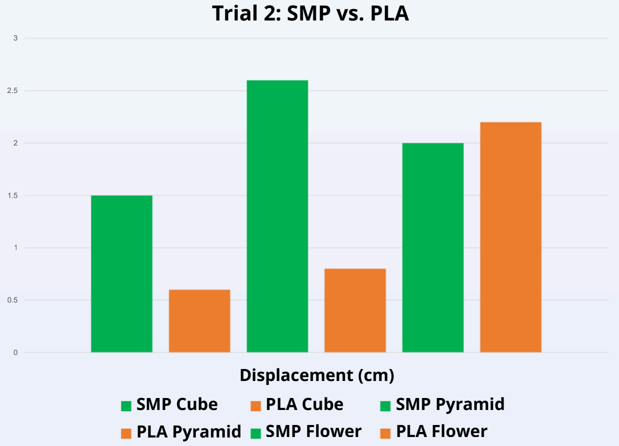

In Trial 2, a similar trend is observed. SMP continues to show higher recovery across all geometries, while PLA exhibits reduced and more inconsistent displacement. The gap between materials remains evident, particularly as conditions vary, reinforcing SMP's ability to maintain performance.

ACKNOWLEDGEMENTS

We would like to thank the MinerSpark mentors for their guidance and support throughout the project, ensuring consistent progress and helping facilitate the research process. We also acknowledge the GAIA Lab at UTEP for providing access to 3D printing resources and technical support.

CONCLUSION

The results demonstrate a clear difference between the behavior of SMP and PLA under thermal and mechanical conditions. SMP functions as a true smart material, consistently recovering its original shape when heated (~60–65°C) while maintaining structural integrity under applied loads. Its repeatable performance across geometries highlights its reliability for applications requiring controlled and predictable shape change. In contrast, PLA behaves as a conventional thermoplastic; although it softens under heat and may exhibit partial recovery, the response is inconsistent and highly dependent on geometry. Under increased load and temperature, PLA showed permanent deformation and surface damage, limiting its effectiveness in repeated or load-bearing applications.

The effect of the tested variables further emphasizes these differences. Increasing load reduced recovery in both materials; however, SMP retained functional recovery and structural stability, while PLA performance degraded significantly. Overall, these findings indicate that SMP is significantly more efficient than PLA for 4D printing applications. SMP provides reliable shape recovery, better performance under load, and repeatability across cycles, whereas PLA is more suitable for low-cost prototyping rather than use as a final smart material. Therefore, SMP is the better material for real-world 4D printing applications due to its ability to consistently recover shape and maintain performance under stress.

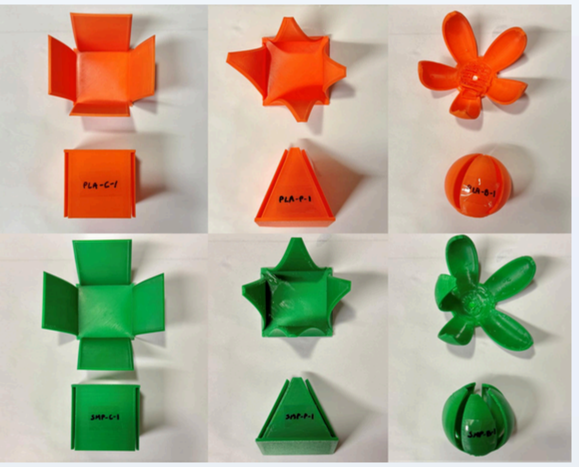

REFERENCES

"4D Printing." ***MIT Media Lab***, Massachusetts Institute of Technology, https://www.media.mit.edu/publications/4d-printing/.

"Researchers 4D Print Tube-Like Soft Robot Capable of Rolling and Climbing on Its Own." ***3D Printing Industry***, https://3dprintingindustry.com/news/researchers-4d-print-tube-like-soft-robot-capable-of-rolling-and-climbing-on-its-own-197409/.

"4D Printing of Shape Memory Polymers for Advanced Functional Applications." ***Advanced Functional Materials***, Wiley Online Library, https://advanced.onlinelibrary.wiley.com/doi/full/10.1002/adfm.201805290.

"Recent Advances in 4D Printing Materials and Applications." ***Advanced Functional Materials***, Wiley Online Library, https://advanced.onlinelibrary.wiley.com/doi/full/10.1002/adfm.202400161.

Q&A

Team 3

THE UNIVERSITY OF TEXAS AT EL PASO
Miner Spark Symposium 2026

Experimental Evaluation of Wireless Relay Node Systems for Communication Reliability in Obstructed Environments: A Study for Search and Rescue Robotics

DominicHernandez • JoseOsuna • JesseRodriguez•ManuelRodriguez

INTRODUCTION

The Problem: Search and Rescue (SAR) robots are essential for hazardousenvironments, yet they are limited by a critical failure:**Wireless Communication.**Common rubble, concrete, rebar, and waterblocks the vital signals needed for these robots tooperate ef fe ct i vel y.
Why: Disaster environments severely degrade wireless communication, limiting the effectiveness of search-and-rescue robots. This project investigates how signal loss occurs and how relay-nodesystems can restore connectivity, enabling safer and morereliable roboticassistancefor first responders.

OBJECTIVE

This study evaluates howwirelessrelay-node deployment affects communication reliability for search-and-rescue robots operating in obstructed environments. Specifically, we aim to:

- **Quantify**signal degradation (RSSI, packet loss, latency, video FPS) as a function of distance and obstructing material just like in search and rescue environments.
- **Measure**the performance gain provided by deploying relay nodes between the operator and edge robot, in this case we used two relay nodes for testing.
- **Establish**practical deployment thresholds. Distance limits, RSSI cutoffs, and material-based range estimates that first responders can apply in real disaster scenarios.

HYPOTHESIS

Wehypothesize that deploying wireless relay nodes will extend the reliable communication range of a search-and-rescue robot beyond the direct-link limit of 35 m. Specifically, one relay will maintain packet loss below 10% and RSSI above −70 dBm out to 60 m, and two relays will sustain real-time video of at least 28 FPS and latency under 150 msacross the same range even through common obstructing materials such as drywall and concrete.

METHODOLOGY

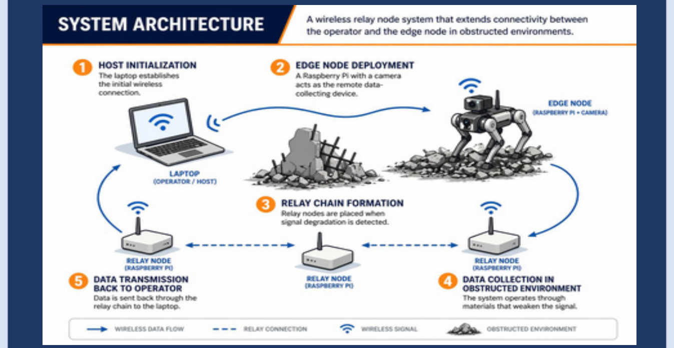

RESULTS

Fig. 1 –RSSI (Signal Strength) vs Distance

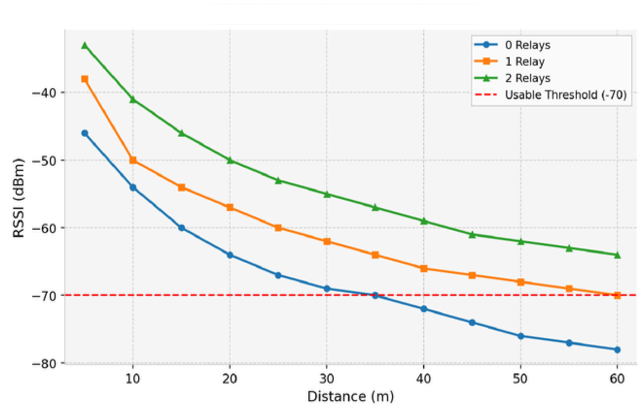

Fig. 2 –Packet Loss vs Distance

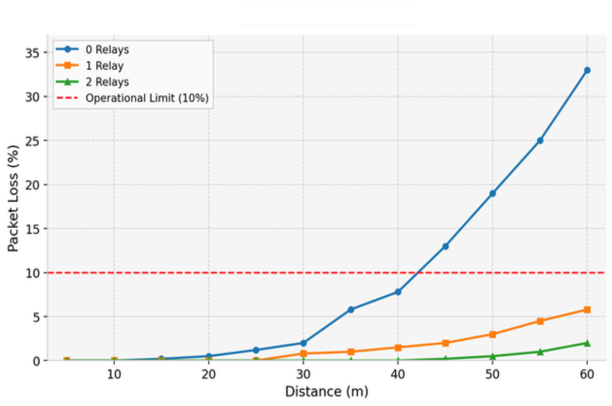

Fig. 3 –Latency vs Distance

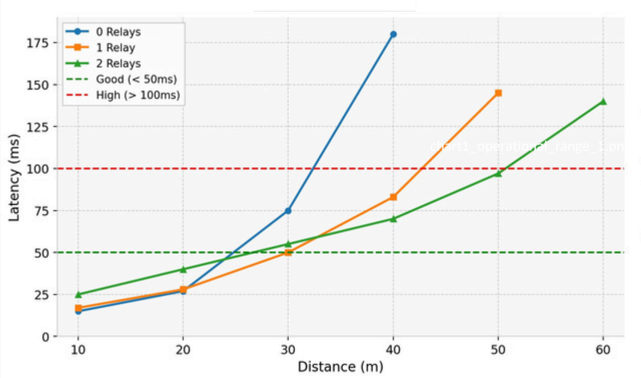

Fig. 4 –Video vs Distance

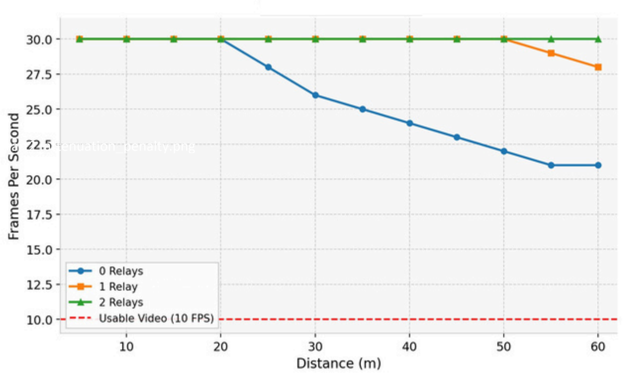

Fig. 5 –Operational Range Threshold

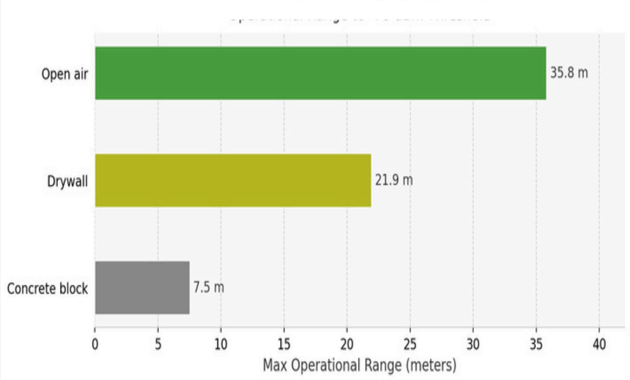

Fig. 6 –Calculated RSSI Degradation vs Distance

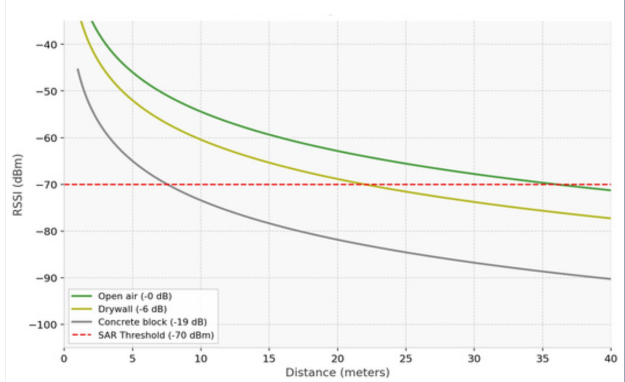

ANALYSIS

Signal Strength (Fig. 1):RSSI degrades inverselywith distance. The direct link crosses the −70 dBm usability threshold at 35 m, while each relay shifts the curve upward by 8–13 dB. With two relays, RSSI at 60 m (−63 dBm) matches the direct-link value at just 25 m.

Packet Loss (Fig. 2): Direct-link loss grows non-linearly past 30 m, exceeding the 10% operational limit by 38 m and reaching 34% at 60 m. One relay holds loss below 6%, two relays stays at or below 2%

Latency (Fig. 3): Direct round-trip time spikes from 75 msat 30 m to 180 msat 40 m, then times out. Each relay hop adds a fixed 6–7 msbut preserves connectivity,two relays maintain 140 msat 60 m where the direct link has failed.

Video (Fig. 4): Direct FPS degrades after 25 m to 21 FPS at 60 m. Both relay configurations hold at least 28 FPS, with two relays steady at 30 FPS.

Material Attenuation (Fig. 5–6): Range to −70 dBm drops from 35.8 m (open air) to 7.5 m (concrete) and 2.6 m (concrete + metal). Empirical ranges align with the modeled curves, validating the attenuation coefficients for deployment planning.

DISCUSSION

The results confirm thatwirelessrelaynodessignificantlyextendcommunication range in obstructed environments. Eachrelayhop adds measurable signalrecovery, with two relays supporting reliable connectivityupto60macrossmostmaterialtypes. The non-linear increase in packet loss and latency spikes seen in direct-link configurations highlight the critical failure points that relays mitigate. Material attenuation coefficients derived from empirical data align closely with theoretical models, reinforcing the validity of the method. These findings suggest that deploying even a single relay node can meaningfully improve SAR robot operability in rubble-filled environments.

CONCLUSION

Wirelessrelay node systemsshow clearperformancegains forSARcommunication in obstructed environments. Signal strength, packet loss, latency, and video quality all improve with relay deployment, particularly at distances beyond 30 m. Two-relay configurations maintained video above 28 FPS and packet loss below 2% across most materials tested. Operational range thresholds varied from 2.6 m (concrete + metal) to 35.6 m (open air) providing actionable deployment guidelines for first responders. Future work should explore dynamic relay placement and real-time adaptive routing in live disaster scenarios.

Quick-Start Field Guide: Relay Node Deployment

Step 1 –Assess theEnvironment Identifyobstructingmaterialsandestimate relay nodes needed based on operationalrangethresholds.
Step 2 –Set Up the Edge Node Position the operator node at command post and confirm logging software is running.
Step 3 –Deploy First Relay Place relay within 30 m of operator. Confirm RSSI stays above –70 dBm.
Step 4 –Advance Robot & Deploy Second Relay If exceeding 30 m or heavy materials, deploy second relay to maintain signal quality.
Step 5 –Monitor in Real Time Watch RSSI, packet loss, latency, and video FPS. Reposition relay if signal drops.

LITERATURE CITED

1. 1.Jais, M. I., Sabapathy, T.,Jusoh, M.,Ehkan,P.,Murukesan, L., Ismail, I., & Ahmad, R. B. (2016). Received signal strength indication (RSSI) code assessment for wireless sensors network(WSN) deployed Raspberry-Pi. *2016 International Conference on Robotics, Automation and Sciences (ICORAS)*, 1–4.
2. Rappaport,T.S.(2002).*Wirelesscommunications:Principles and practice*(2nd ed.). Prentice Hall.
3. Liu,J., & Hu, Y. (2007). A review of search-and-rescue robot research. *International Journal of Advanced Robotic Systems*, 4(4), 1–10.
4. Agha-mohammadi, A., Chakravorty, S., & Amato, N. (2022). NeBulaautonomy: Advanced robotic autonomy for subterranean exploration. *Journal of Field Robotics*.
5. Vujović, V., & Maksimović, M. (2014). Raspberry Pi as a wireless sensor node: Performances and constraints. *2014 37th International Convention on Information and Communication Technology, Electronics and Microelectronics (MIPRO)*, 1247–1252.
6. Zeng, H., & Kang, Z. (2017). Relay node placement to restore connectivity in wireless sensor networks. *2017 IEEE 9th International Conference on Communication Software and Networks (ICCSN)*, 301–305.
7. Sudhakar, A., & Madhavi, D. (2017). Analysis and measurement of attenuation constants of ultra widebandsignal through commonly used building materials. *2017 Progress in Electromagnetics Research Symposium (PIERS)*, 161–164.
8. Cirstea, C., Cernaianu, M., & Gontean, A. (2012). Packet loss analysis in wireless sensor networks routing protocols. *2012 35th International Conference on Telecommunications and Signal Processing (TSP)*, 37–41.

ACKNOWLEDGEMENTS

We thank the Miner Spark Symposium for the opportunity to present this work, and our faculty mentors Lizbeth Liceroand Rosario Lara for their guidance throughout the project. We are also grateful to the UTEP SHPE/MAES chapter for their support, and to the CREATE program for providing the resources and testing space that made this research possible.

Q&A

CENTER FOR RESEARCH IN
ENGINEERING
AND TECHNOLOGY
EDUCATION

SHPE // MAES
UNIVERSITY OF TEXAS
AT EL PASO

THANK YOU

Keep shining